[3] Lo H, Crate, H and Schwartz, E B "Buckling of thin-walled cylinders under axial compression and internal pressure," NACA TN 2021 (January 1950)

[4] von Kármán, T and Tsien, H-S, 'The buckling of thin cylindrical shells under axial compression, J Aeronaut Sci **8**, 303–312 (1941)

[5] Holmes, M, 'Compression tests on thin-walled cylinders," Aeronaut Quart **12**, 150–164 (February–November 1961)

[6] Fung, Y C and Sechler, E E, 'Buckling of thin-walled circular cylinders under axial compression and internal pressure," J Aeronaut Sci **24**, 351–356 (1957)

[7] Fung, Y C and Sechler, E E, "Instability of thin elastic shells," *Structural Mechanics*, edited by J N Goodier and N J Hoff (Pergamon Press, New York, 1960), pp 115–168

Experimental Measurement of Pitot Pressure in the Boundary Layer on a Model in a Hypersonic Gun Tunnel

A J Cable*

The War Office, Royal Armament Research and Development Establishment, Fort Halstead, England

RECENT interest in hypersonic boundary layers has led to the development of instrumentation to measure the pitot pressure in the boundary layer on a model in the (Royal Armament Research and Development Establishment) no 3 Hypersonic Gun Tunnel,[1] which, at its present stage of development, is capable of simulating both full scale Mach numbers and Reynolds numbers for quite large vehicles The flow duration in this tunnel is of the order of 40 msec

The model chosen for exploratory testing was a flat plate with a hemicylindrical leading edge ($\frac{1}{8}$-in radius) that had previously been pressure plotted The model with the small pitot tube for boundary-layer measurements is shown in Fig 1 The pitot was constructed of flattened hypodermic tubing measuring 0 022 in × 0 018 in externally and 0 011 in × 0 009 in internally The tube was brazed to a body containing a Statham type PM 222 TC transducer The body could be moved inside the model to position the pitot tube in the boundary layer from a point 0 1 in from the surface of the model to flush with the surface

The model was tested at a Mach number of 8 4, and the Reynolds number at the pitot position was $6\,2 \times 10^6$ based on freestream conditions and its distance from the leading edge For some of the tests, an externally mounted pitot tube was also used to measure the pitot pressure in the region between the bow shock wave and the limit of movement of the internally mounted pitot tube The boundary layer was traversed at 0 01-in intervals by the internal pitot and at approximately $\frac{1}{4}$-in intervals with the external pitot

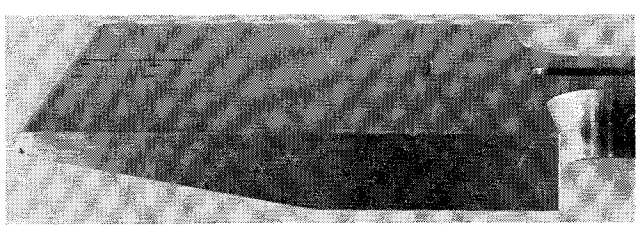

Fig 1 Model showing boundary-layer pitot

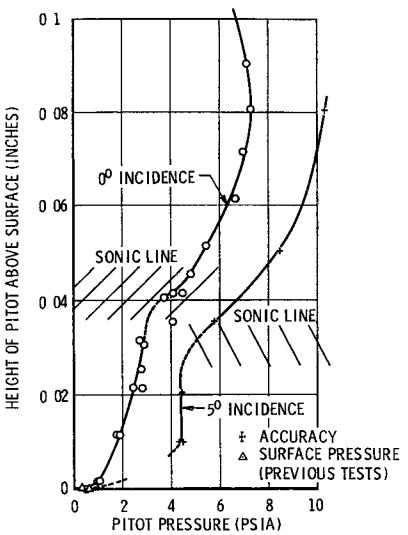

Fig 2 Pitot traverse close to model surface

Figure 2 shows the distribution of pitot pressure in the region between the surface and 0 1 in from the surface for the model at zero and 5° incidence Also indicated are the surface pressures measured in previous tests In each case the surface pitot pressure is close to the surface static pressure It can be seen that the measurements are repeatable except for the region around 0 04 in from the surface at zero incidence On examining schlieren photographs (Fig 3), it was noticed that the shock wave caused by the small pitot tube ended abruptly at about this height This indicated the position of the sonic line in the boundary layer, and it is considered that the nonrepeatability of measurements in this region was caused by the flow being choked locally by the presence of the pitot tube Since the position cannot be measured to a greater accuracy than ±0 005 in from the photographs, the sonic line is shown hatched in Fig 2 A similar effect occurs at incidence but at a lower height

The pitot pressure distribution in the flow between the model surface and bow shock wave (Fig 4) shows that there is a region where the pitot pressure does not vary with height above the surface (0 1–0 4 in at zero incidence) On examining schlieren photographs (e g, Fig 3), it can be seen that this region corresponds to a light region with ill-defined edges This has been interpreted as the entropy layer in previous tests,[2] and a similar interpretation is plausible in this case The extent of the region measured from the schlieren photo-

Fig 3 Schlieren photograph of model at $M = 8\,4$

Received January 13, 1964 British Crown Copyright reserved Published with the permission of the Controller of Her Britannic Majesty's Stationery Office

* Now Supervisor, Launcher Systems Section, von Kármán Gas Dynamics Facility, ARO, Inc (contract operator of the Arnold Engineering Development Center Air Force Systems Command, under U S Air Force Contract No AF 40(600)-1000) Member AIAA

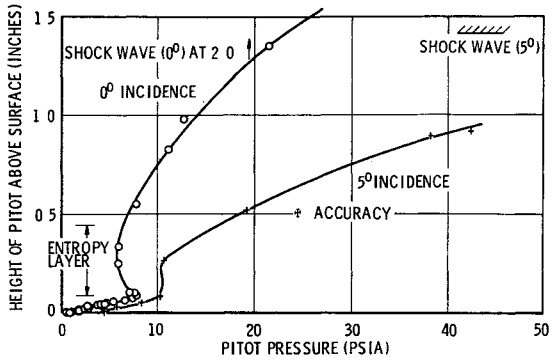

Fig 4 Pitot traverse between model and shock wave

graphs is shown on Fig 4 and corresponds closely with the region of constant pitot pressure

The position of the internally mounted pitot is accurate to ±0 001 in and that of the externally mounted tube to ±0 02 in The pressures are measured to an accuracy of ±0 1 psi

It has been shown that it is possible to measure the pitot pressure in the boundary layer on a model in the running time of a hypersonic gun tunnel (40 msec) Other results, which call for further investigation, are the identification of the sonic line in the boundary layer and the boundary of entropy layer

References

[1] Cox, R N and Winter, D F T, "Hypersonic flow," *Proceedings of the 11th Symposium of the Colston Research Society* (Royal Armament Research and Development Establishment, Bristol, 1959), pp 111–141

[2] Wood, N B, 'Nose bluntness effects on cone pressure and shock shape at $M = 8\,5$ to $12\,9$,' AIAA J **1**, 1929–1930 (1963)

Analysis of Air Arc-Tunnel Heat-Transfer Data

DANIEL E ROSNER*
AeroChem Research Laboratories, Inc , Princeton, N J

Nomenclature

c_p = specific heat of mixture
D_i = Fick coefficient for diffusion of species i through the mixture
h = specific enthalpy (including chemical contributions)
k = Boltzmann constant
$k_R(T)$ = termolecular (homogeneous) atom recombination rate constant at temperature T ($dn_i/dt = -2k_{R\,i}n_i^2n$)
$k_{w\,i}$ = $(m_in_{i\,w})^{1-n}[kT_w/(2\pi m_i)]^{1/2}\gamma_i$
Le_i = Lewis number $\equiv D_i/[\lambda_f/(\rho c_{p\,f})]$
m_i = mass of species i
n = true reaction order
n = number density (p/kT)
N = number of thermochemical energy carriers
p = pressure
Pr = Prandtl number for heat conduction $\equiv (\mu/\rho)/[\lambda_f/(\rho c_{p,f})]$
Pr_D = Prandtl number for diffusion $\equiv(\mu/\rho)/D_i$
$\dot{q}$ = calorimeter heat flux
$r_{D\,i}$ = recovery factor for chemical energy[3] associated with species i; $r_{D\,i} = (Le_i)^{0.6}$ for stagnation-point boundary layer
$St_{D\,i}$ = local Stanton number for convective transport of species i
T = absolute temperature
u = component of gas velocity parallel to surface
$z^{(G)}$ = generalized gas-phase recombination parameter Eq (4)
$z_i^{(W)}$ = $k_{w\,i}\rho_w(\rho_w\alpha_i)^{n-1}/(\rho\, u\, St_{D\,i})$
α_i = mass fraction of species i in the mixture
γ = heterogeneous recombination coefficient (probability that an atom incident upon the surface will recombine)
λ = thermal conductivity of gas mixture
μ = dynamic viscosity of mixture
ρ = mass density of mixture
ϕ_i = extent of recombination for species i; $\phi_i = \Delta h_{\mathrm{hm}\,i}/\Delta h_{\mathrm{hm}\,i\,\mathrm{max}}$
Δ = operator meaning change in (across boundary layer)

Subscripts

chem = chemical contribution
e = at outer edge of boundary layer
eq = pertaining to local thermochemical equilibrium
f = chemically frozen
i = pertaining to species i
min = minimum value (no recombination)
max = maximum value (complete recombination)
w = at wall
1 = pertaining to atoms in a binary mixture

Received January 16, 1964 This work was supported by the Propulsion Division of the Office of Aerospace Research, U S Air Force Office of Scientific Research, under Contract AF 49 (638) 1138 This paper is a revised version of AeroChem TP 76 (January 2, 1964)

* Aeronautical Research Scientist Associate Fellow Member AIAA

Introduction

WETHERN[1] has compared data on subsonic air arc-tunnel heat transfer to a water-cooled copper calorimeter with the predictions of several limiting theoretical models end concluded that the assumptions of chemically frozen boundary-layer flow and a noncatalytic wall were virtually exact for most of the conditions studied Since a copper surface can behave this way at stagnation pressures and enthalpies approaching 1 atm and 10^4 Btu/lbm, respectively, calorimeter catalytic activity becomes an important parameter, particularly if effective heats of ablation or total enthalpies are subsequently to be determined from heat-transfer data obtained at thermally significant dissociation levels In this note, a direct procedure for estimating catalytic activities from such calorimeter heat-transfer data is illustrated, and a prediction is made of the stagnation pressure levels at which gas-phase atom recombination should mask the observed effects of calorimeter surface specificity under arc-tunnel conditions Implications of this result for materials testing, and factors governing the probability of atom recombination on metal and metal oxide surfaces, are briefly discussed in the light of recent kinetic observations

General Theory

It is a short step to go from limiting heat fluxes (i e , predictions or data giving $\dot{q}''_{\max}$ and $\dot{q}''_{\min}$) and calorimeter heat flux data of the type presented in Ref 1 to quantitative estimates of the relevant atom recombination probabilities, particularly when the stagnation pressure level and calorimeter size are sufficiently small so that gas-phase atom recombination (in the boundary layer) can be neglected † Applying the methods exploited in Refs 2 and 3, one can readily show that

$$\frac{\dot{q}'' - \dot{q}''_{\min}}{\dot{q}''_{\max} - \dot{q}''_{\min}} = \frac{\sum_{i=1}^{N} \phi_i r_{D\,i}\Delta h_{\mathrm{chem}\ i\ \max}}{\sum_{i=1}^{N} r_{D\,i}\Delta h_{\mathrm{hem}\ i\ \max}} \qquad (1)$$

† See section entitled "Gas-Phase Recombination"